

Shielding Effectiveness Estimation of Enclosures with Apertures

I. Belokour

Department of Electrical Engineering,
The University of Western Ontario,
London, Ontario, N6A 5B9, Canada
belokour@engga.uwo.ca

J. LoVetri

Department of Electrical Engineering,
The University of Manitoba, Winnipeg,
Manitoba R3T 5V6, Canada
lovetri@ee.umanitoba.ca

S. Kashyap

Department of National Defence,
Defence Research Establishment,
Bldg. 29, 3701 Carling Ave., Ottawa,
Ontario, K1A 0K2, Canada

Abstract

A curve fitting technique has been used to develop a "phenomenological" model based on numerically collected data for the coupling of electromagnetic energy through apertures into enclosures. It has been shown elsewhere that a simple transmission line formulation predicts well the shielding effectiveness of a rectangular enclosure with apertures. The finite difference time-domain method is used for computing electromagnetic fields within the enclosure with apertures. The investigation is focused on the estimation of shielding effectiveness depending on the number of apertures, their area, test point location within the enclosure as well as the incidence angle and polarization of the electromagnetic field impinging on the enclosure. The obtained results allow estimation of the shielding effectiveness at the enclosure design stage.

Introduction

It is difficult to meet electromagnetic compatibility (EMC) requirements for many electronic products without shielding enclosures [1]. However, the integrity of shielding enclosures is often compromised by apertures and slots used to accommodate visibility, ventilation or access to interior components. Such openings allow exterior electric and magnetic fields to penetrate to the interior space, where they may couple onto printed circuit boards (PCBs) thus inducing current and voltage on interior conductors.

EM penetration as well as radiation from conducting enclosures and cavities below cavity-mode resonances has been investigated experimentally and numerically [2], [3], [4], [5].

Recently, an attempt has been made for estimating the shielding effectiveness (SE) of an empty rectangular enclosure with a rectangular aperture by using a simple transmission line (Tx-line) formulation [7]. The enclosure is considered as a waveguide with a single mode of propagation. A rectangular aperture in an empty rectangular enclosure is represented by the equivalent circuit of Robinson *et al.* [8]. The electric shielding at a distance p from the slot is obtained from the voltage at point P in the equivalent circuit [8], while the current at P gives the magnetic shielding. However, this formulation is limited

by the assumption of a single mode and does not consider the incidence angle or polarization of the impinging EM field. The variation of SE due to the mutual admittance between apertures in aperture arrays is also of interest in designing the perforation patterns for airflow. This motivated further numerical investigation with the objective to extend the applicability of the Tx-line model.

A "phenomenological" model based on numerically collected data for the coupling of EM energy through apertures, slots or seams into enclosures used for SE estimation is reported herein. The purpose of this model is to predict the SE of enclosures with apertures at the design stage which is important for the susceptibility evaluation of an electronic system.

The FDTD Model Geometry

The finite difference time domain (FDTD) technique has proven to be a very promising method for time-domain analysis of any volumetric structure with rectangular cells. It has been described in detail in [9].

FDTD objects are defined by specifying dielectric and magnetic material parameters at the calculated electric and magnetic field locations. The computational domain must be large enough to enclose the object. In addition, suitable boundary conditions on the numerical boundary must be imposed to simulate the extension of the computational domain to infinity. To ensure the stability of the FDTD scheme, the time increment, Δt , must satisfy the Courant stability condition [9]

An FDTD code utilizing the scattering formulation [10] has been developed at *The University of Western Ontario, Canada*. It was employed to compute the SE of a rectangular enclosure with apertures as well as the electric and magnetic field distributions inside it. The rectangular enclosure with an aperture is shown in Figure 1. A rectangular three-dimensional grid of 140 x 140 x 68 cells is used as the computational domain. Spatially, the computational domain is discretized so that the largest grid dimension is less than about a sixteenth of the shortest wavelength of interest. A higher resolution was chosen to more accurately model apertures associated with this configuration. The spatial increments in the x , y , and z directions are

$\Delta x = \Delta y = \Delta z = 2.5\text{mm}$. The time step associated with this spatial increment dimension is $4.81 \cdot 10^{-9}$ s.

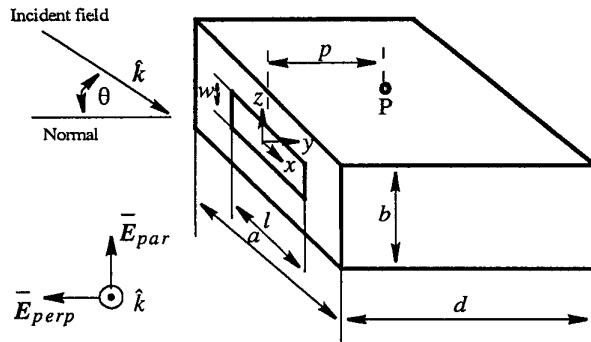


Figure 1. Rectangular enclosure with a slot

The enclosure walls are defined to be infinitely thin and perfectly conducting, *i.e.*, the tangential electric field components on these planes are forced to be zero. The front side has a single-centered l by w slot. Absorbing boundary conditions must be applied at the outer boundary of the computational domain in order to simulate unbounded space. Since external fields around the sides of the enclosure are not important, Mur's first-order boundary conditions are used for efficiency [11].

The source of excitation is a plane uniform Gaussian pulse normally incident on the front face of the enclosure with the aperture. The incident electric field has a spatial variation in y -direction given by a Gaussian pulse. The source of excitation and its Fourier transform are shown in Figure 2 and Figure 3 respectively. The longer side of the slot is normal to the E -field which is the worst case for shielding. The SE is determined at the test location P along the center line within the enclosure.

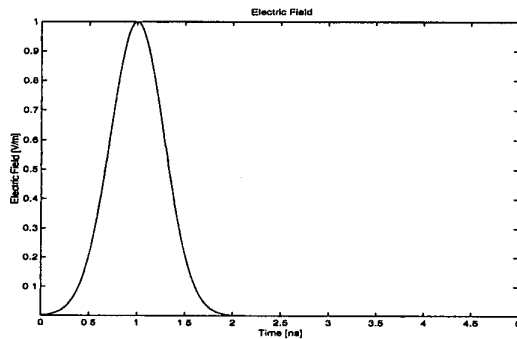


Figure 2. Incident field

The FDTD simulations were executed until the steady state was reached, which for excitations with pulse-time profiles occurs when the fields in the computational domain have

become negligibly small. The simulations typically required from 4000 to 6000 time steps to achieve the steady state. The simulation required about 40 MB of computer memory and ran for 17 hours. Hanning windowing was used to smooth the obtained data before a Fourier transform was applied to the data to obtain frequency-domain information.

The FDTD simulation results were validated by comparing with that obtained for the Tx-line model [7]. The SE obtained via the models at the incidence angle $\theta = 0$ and parallel polarization is shown in Figure 4. The agreement is reasonably good. (Note the beginning of a second resonance predicted by FDTD.)

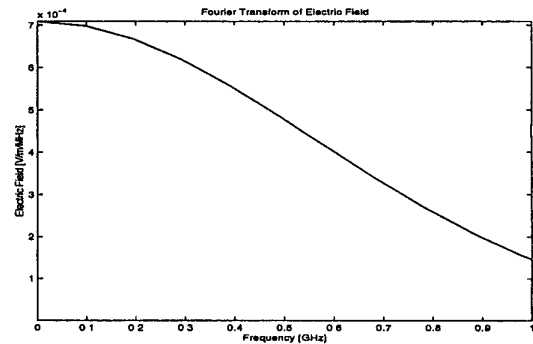


Figure 3. Fourier transform of the incident field

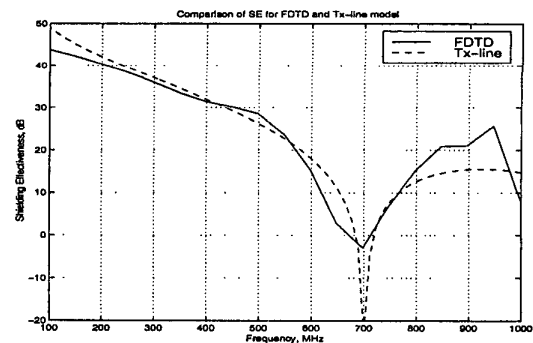


Figure 4. SE for FDTD and Tx-line models at normal incidence and parallel polarization.

Incidence and Polarization Angle Estimates

To extend the Tx-line model applicability, we need to consider the SE variation in terms of the incidence and polarization angle. To this end, let us consider how different aperture and enclosure dimensions and a test point location within the enclosure affect the SE.

For electrically small apertures, at frequencies below the aperture fundamental resonance, the Bethe small-hole theory [12] states that the transmitted fields are those of induced normal electric and tangential magnetic dipole moments

$$p_m = \alpha_m H_{\tan}^{sc} \quad \text{and} \quad p_e = \alpha_e \epsilon_0 E_n^{sc} \quad (1)$$

where H_{\tan}^{sc} is the tangential magnetic field at the center of the short-circuited aperture and E_n^{sc} is the normal electric field at the center of the short-circuited aperture, α_m and α_e are the electric and magnetic polarizabilities. The electric and magnetic polarizabilities for a slot of length l and width w can be found in [13]. For parallel polarization, the short-circuited fields are [2]

$$H_{\tan}^{sc} = 2H_i \quad \text{and} \quad E_n^{sc} = 2E_i \sin \theta^i \quad (2)$$

For perpendicular polarization, the short-circuited fields are

$$H_{\tan}^{sc} = 2H_i \cos \theta^i \quad \text{and} \quad E_n^{sc} = 0 \quad (3)$$

where θ^i is the incidence angle.

The total transmitted power for dipoles radiating in the presence of the ground plane is [2]

$$P_t = \frac{4\pi\eta_0}{3\lambda^2} (k^2 |p_m|^2 + |\omega p_e|^2) \quad (4)$$

where η_0 is the intrinsic impedance of a medium, λ is the wavelength, k is the wavenumber, and ω is the frequency. One can see from (2) and (3) that the fields coupled into the enclosure depend on the incidence and polarization angles. Applying the Babinet's principle we can reduce (4) to antenna problems [1]. Indeed, considering a slot as an infinitely narrow dielectric gap, we can substitute the slot with an equivalent infinitely thin antenna.

The transition between free-space and waveguide in the Tx-line model is represented by considering the aperture as a length of a coplanar strip transmission line, shorted at each end. The total width is equal to the height of the enclosure b and the separation is equal to the width of the aperture w . The aperture characteristic impedance is given in [7]. More than one individual aperture impedance can be combined taking into account their mutual admittances if apertures are in the same face of the enclosure.

A shielded enclosure has resonances associated with its dimensions. The interior fields for a TM_z (mnp) mode for an ideal rectangular cavity are given in [14]. At the same time, it was found in [4] and confirmed by the FDTD simulations that aperture dimensions do not appreciably change enclosure mode resonances. One can come to a conclusion by analyzing (4) that the incidence and polarization angle variations do not affect appreciably the spectrum inside the enclosure. This fact is confirmed in Figure 4 - Figure 10 by FDTD simulations.

The SE variations for the angle increment of 10 degrees were obtained by FDTD simulations for the range of incidence angles from 0 to 80 degrees for both polarization angles (parallel and perpendicular). The obtained array of SE data for incidence angles was normalized by the SE for normal incidence while the array of SE data for polarization angles was normalized by the SE for parallel polarization. Thus, the dependence on a test point location within the enclosure was reduced significantly. Then the array of SE_{nor} was fitted with a polynomial of order 6 in the least squares sense. The SE variation caused by a test point location within the enclosure was significantly reduced by using the normalized shielding effectiveness SE_{nor} explained in detail in the next section. The obtained polynomial coefficients given in Table 1 were used in the Tx-line model to provide for the estimate of the SE variation caused by a variation in incidence or polarization angle.

The results obtained for various incidence angles are shown in Figure 4 - Figure 7. It can be seen that the SE increases by increasing the incidence angle in relation to normal incidence of the EM field.

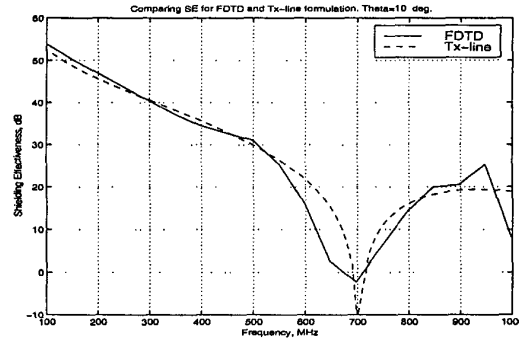


Figure 5. SE for FDTD and Tx-line models at incidence angle 10 degrees and parallel polarization.

Table 1. The polynomial coefficients of descending power.

| | | | | | | | |
|--------------------|-----------|------------|-----------|------------|-----------|-----------|------------|
| Polarization model | 1.3210e-1 | -2.4240e-1 | 1.1123e-1 | -2.3274e-1 | 2.7375e0 | -3.1178e0 | -6.6486e-1 |
| Incidence model | -5.6361e0 | -2.9929e0 | 1.4877e1 | 8.6617e0 | -8.7343e0 | -6.2890e0 | 3.4395e-1 |

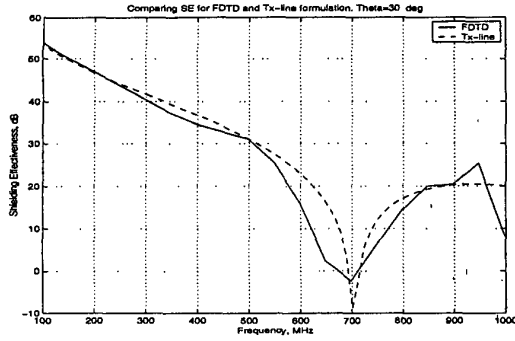


Figure 6. SE for FDTD and Tx-line models at incidence angle 30 degrees and parallel polarization.

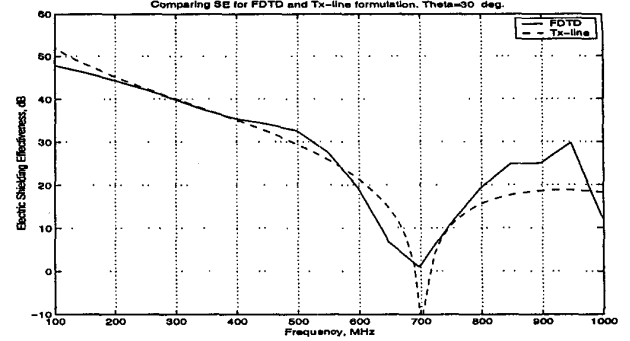


Figure 9. SE for FDTD and Tx-line model at normal incidence angle and polarization angle 30 degrees.

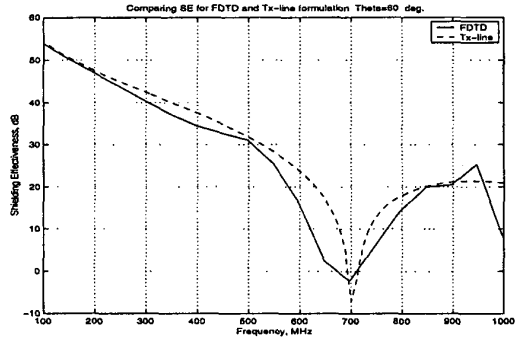


Figure 7. SE for FDTD and Tx-line models at incidence angle 60 degrees and parallel polarization.

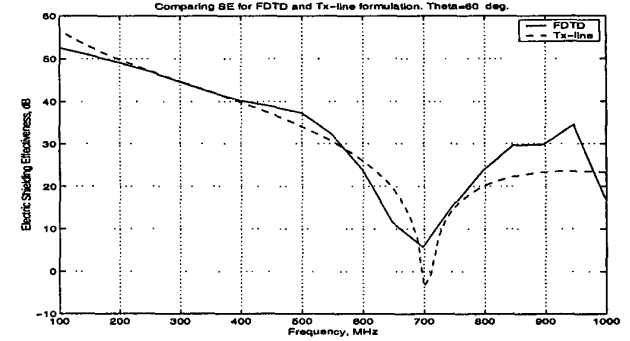


Figure 10. SE for FDTD and Tx-line model at normal incidence angle and polarization angle 60 degrees.

The results obtained for various polarization angles are shown in Figure 8 - Figure 10. And again the agreement is good.

Shielding effectiveness of an enclosure with various combinations of apertures

Aperture arrays or combinations of apertures are often used for airflow in shielding enclosures. The empirical relation for the relative radiation of four different perforation patterns normalized to the radiation from the 1cm x 1cm perforation pattern is given in [15] as

$$E_{far} \sim d^3 \sqrt{N} \quad (5)$$

where d is aperture diameter, and N is the number of apertures. However, further simulations on single apertures in the middle of the front enclosure face performed in [4] showed that the relative radiation for the scale factor N is generally 3 dB above the radiation from the corresponding perforation pattern. It was suggested that the 3 dB difference might be explained by the effect of the electric field variation over the footprint of the perforation patterns, while the single aperture from the center of the front pattern is at the maximum tangential magnetic field and normal electric field position for the cavity modes studied. The N factor instead of \sqrt{N} was reasonably adopted.

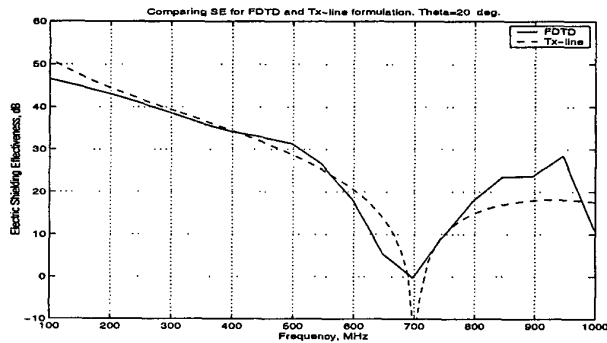


Figure 8. SE for FDTD and Tx-line model at normal incidence angle and polarization angle 20 degrees.

The minimum value of SE corresponds to the parallel polarization of the incident EM field. The SE increases as the polarization changes from parallel to perpendicular.

It was also assumed in [7] that if there are n similar apertures in one face of the enclosure, then the individual impedances may simply be combined in series according to

$$Z_{ap} = 0.5jn(l/a)Z_{0s}\tan(kl/2) \quad (6)$$

where n is the number of apertures.

To this end a 100 mm by 5 mm aperture was divided into several shorter apertures. Measurements showed that having more but smaller holes improves the SE. The agreement was within 2-6 dB. However, this approach ignores the mutual admittances between apertures and is not applicable if the apertures are too close together.

FDTD simulations were performed to validate the above assumption and to compare with the results obtained in [4] and [15].

In order to estimate the SE reduction caused by apertures spaced too close together the SE of an enclosure provided with two 50 mm by 5 mm centered side by side apertures separated by the 5 mm and 55 mm spacing respectively was simulated. The results obtained are shown in Figure 11. One can see the 2 dB reduction in SE for the case of a 5 mm spacing between apertures compared to the SE for the case of a 55 mm spacing between apertures. The obtained SE was normalized by that for a single 50 mm by 5 mm aperture.

Simulations were performed to estimate the variation in SE as a function of the number of apertures. Shielding can be specified in terms of the reduction in magnetic and/or electric field strength caused by the shield. Shielding effectiveness (SE) is defined in [6] for electric fields as

$$S_E = 20\log E_i/E_t \quad (7)$$

and for magnetic fields as

$$S_M = 20\log H_i/H_t \quad (8)$$

where E_i or H_i is the incident field strength, and E_t or H_t is the field strength of the transmitted wave as it emerges from the shield. However, an estimate based on the comparing of the field strength at a test point within an enclosure with that of a plane wave illuminating the enclosure is not a fair way since in this case SE depends on the exact position of the test point within the enclosure. It is better to use the estimate based on a normalized shielding effectiveness SE_{nor} , given as

$$SE_{nor} = SE/SE_{ref} \quad (9)$$

where SE is the shielding effectiveness of an array of apertures and SE_{ref} is the shielding effectiveness of a single aperture correspondingly.

Thus, one can compare the penetration through apertures in terms of that for a reference aperture, i.e., with each other, at the same test point inside the enclosure. This approach allows different combinations of apertures to be directly compared with one another.

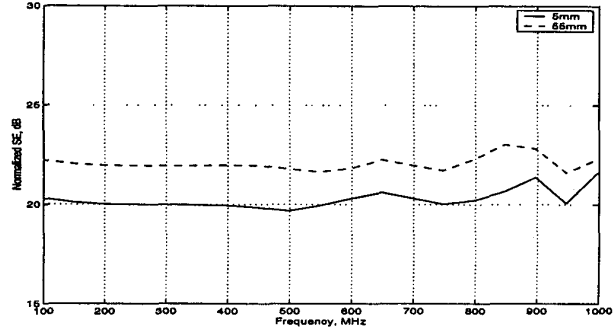


Figure 11. Reduction in SE due to the spacing variation between two apertures.

The SE_{nor} for the combination of apertures obtained by FDTD and Tx-line simulations is given in Table 2. In each case the SE_{nor} was obtained according to (9) by normalizing with the SE for a single aperture while keeping the total perforated area of 500 mm² constant.

Table 2: SE_{nor} vs. the number of apertures

| No. of apertures | SE_{nor} for FDTD simulations | SE_{nor} for Tx-line simulations |
|------------------|---------------------------------|------------------------------------|
| Dimensions, mm | dB | dB |
| Ten 10 by 5 | 15.4 | 19.9 |
| Five 20 by 5 | 23.6 | 25.9 |
| Four 25 by 5 | 22.9 | 27.9 |
| Two 50 by 5 | 33.1 | 33.9 |

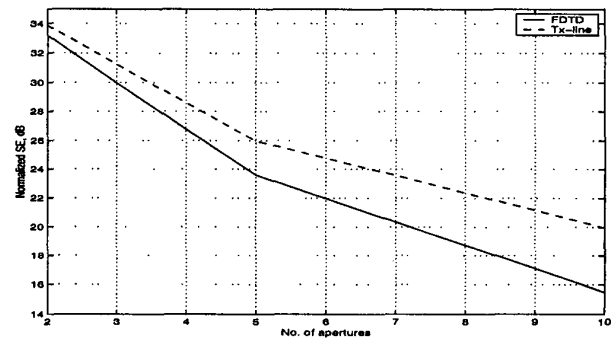


Figure 12. SE_{nor} vs. the number of apertures.

SE_{nor} vs. the number of apertures is given in Figure 12. The results showed that the SE_{nor} for the Tx-line model was above the SE_{nor} for the FDTD simulation. The effect of the width variation on SE_{nor} was suppressed by keeping the aperture width constant. The maximum deviation of about 5 dB was observed for the pattern of ten apertures. This might be caused by the decreased spacing between apertures due to the mutual admittances between apertures.

Conclusions

The SE of a rectangular enclosure has been numerically investigated using the FDTD technique. Good agreement between the results obtained from the Tx-line model and FDTD model have been obtained. The application of the Tx-line model for estimating SE of a rectangular enclosure with apertures has been expanded by incorporating the polarization and incidence angles based on the curve fitting technique.

An estimate of SE variation as a function of the number of apertures has been developed. It can be used in enclosure design for reducing aperture length to achieve the desired SE increase in the frequency range of interest. This estimate is a useful tool for designing and evaluating shielding enclosures.

Application of the expanded Tx-line model gives significant savings in computational time and resources. The obtained results allow estimation of the SE of an rectangular enclosure at the design stage.

References

- [1] A. Tsaliovich, *Electromagnetic Shielding Handbook for Wired and Wireless EMC Applications*, Kluwer Academic Publishers, Boston, 1999
- [2] D.A. Hill, M.T. Ma, A.R. Undertake, B.F. Riddle, M.L. Crawford, and R.T. Johnk, "Aperture excitation of electrically large, lossy cavities", *IEEE Trans. on Electromagnetic Compatibility*, vol. 36, no.3, Aug. 1994.
- [3] C.L. Gardner and P.A. Hrubik, "An Experimental and Analytical Study of the Use of Bounds to Estimate the Coupling to a Monopole Inside a Cavity with an Aperture", *IEEE Trans. on Electromagnetic Compatibility*, vol. 41, no. 1, 1999, pp. 64-74.
- [4] M. Li, S. Radu, J.L. Drewniak, T.H. Hubing, and T.P. VanDoren, R.E. DuBruff, "An EMI Estimate for Shielding Enclosure Design," *13th Int. Zurich Symposium on EMC*, Zurich, 1999.
- [5] J. LoVetri, A.T.M. Wilbers, A.P. Zwamborn, "Microwave interaction with a personal computer: experiment and modeling," *13th Int. Zurich Symp. on EMC*, Zurich, 1999.
- [6] H.W. Ott, *Noise reduction techniques in electronic systems*, Wiley Interscience, 1988, 2nd edn.
- [7] M.P. Robinson, T.M. Benson, C. Christopoulos, J.F. Dawson, M.D. Ganley, A.C. Marvin, S.J. Porter, and D. Thomas, "Analytical Formulation for the Shielding Effectiveness of Enclosures with Apertures," *IEEE Transactions on Electromagnetic Compatibility*, vol. 40, no. 3, 1998, pp. 240-247.
- [8] M.P. Robinson, J.D. Turner, D.W.P. Thomas, J.F. Dawson, M.D. Ganley, A.C. Marvin, S.J. Porter, T.M. Benson and C. Christopoulos, "Shielding Effectiveness of a Rectangular Enclosure with a Rectangular Aperture," *Electronic Letters*, vol. 32, no. 17, 1996, pp.1559-1560.
- [9] K.S. Kunz and R.J. Luebbers, *The Finite Difference Time Domain Method for Electromagnetics*, Boca Raton, FL, CRC, 1993.
- [10] D. Mardare, R. Siushansian, and J. LoVetri, "3-D Dispersive EMFDTD", Version 1.3, The University of Western Ontario, Department of Electrical Engineering, Dec. 1995.
- [11] G. Mur, "Absorbing Boundary Conditions for the Finite-Difference Approximation of the Time-Domain Electromagnetic-Field Equations," *IEEE Trans. on Electromagnetic Compatibility*, vol. EMC-23, pp. 377-382, 1981.
- [12] H.A. Bethe, "Theory of Diffraction by Small Holes", *Physical Review*, vol. 66, no. 7 and 8, 1944, pp. 163-182.
- [13] K.S.H. Lee, ed., *EMP Interaction: Principles, Techniques, and Reference Data*, Hemisphere, Washington, DC.
- [14] C.A. Balanis, *Advanced Engineering Electromagnetics*, John Wiley & Sons, NY, 1989.
- [15] M. Li, S. Radu, J. Nuebel, J.L. Drewniak, T.H. Hubing, T.P. VanDoren, "Design of Airflow Aperture Arrays in Shielding Enclosures", *IEEE Electromagnetic Compatibility Symposium Proceedings*, pp.1059-1063, 1998.